POLITECNICO DI TORINO
Repository ISTITUZIONALE

Metrological Characterization of Sensors for Thermal and Air Quality Parameters: A Case Study on a Multi-Sensor System for Monitoring Indoor Environmental Quality

Original
Metrological Characterization of Sensors for Thermal and Air Quality Parameters: A Case Study on a Multi-Sensor System for Monitoring Indoor Environmental Quality / Russo, R., Bottacin, A., Arcamone, G., Durbiano, F., Musacchio, C., Pavarelli, S., Pellegrino, A., Romana Pennecchi, F., Sega, M., Rolle, F., Favoino, F.. - In: CHEMOSENSORS. - ISSN 2227-9040. - 14:9(2026). [10.3390/chemosensors14090190]

Availability:
This version is available at: 11583/3015272 since: 2026-09-07T13:24:36Z

Publisher:
MDPI

Published
DOI:10.3390/chemosensors14090190

Terms of use:

This article is made available under terms and conditions as specified in the corresponding bibliographic description in the repository

Publisher copyright

(Article begins on next page)

04 November 2026

chemosensors

MDPI

Article

Metrological Characterization of Sensors for Thermal and Air Quality Parameters: A Case Study on a Multi-Sensor System for Monitoring Indoor Environmental Quality

Ramona Russo [1,2,*], Alberto Bottacin [1], Giuseppina Arcamone [2], Francesca Durbiano [1], Chiara Musacchio [1], Stefano Pavarelli [1], Anna Pellegrino [2], Francesca Romana Pennecchi [1], Michela Sega [1], Francesca Rolle [1] and Fabio Favoino [2]

[1] Istituto Nazionale di Ricerca Metrologica (INRiM), 10135 Turin, Italy; a.bottacin@inrim.it (A.B.); f.durbiano@inrim.it (F.D.); c.musacchio@inrim.it (C.M.); s.pavarelli@inrim.it (S.P.); f.pennecchi@inrim.it (F.R.P.); m.sega@inrim.it (M.S.); f.rolle@inrim.it (F.R.)
[2] Department of Energy (DENERG), Politecnico di Torino, 10129 Turin, Italy; giuseppina.arcamone@polito.it (G.A.); anna.pellegrino@polito.it (A.P.); fabio.favoino@polito.it (F.F.)
* Correspondence: r.russo@inrim.it

Abstract

This paper presents the metrological characterization of low-cost sensors integrated into a multi-sensor system for Indoor Environmental Quality monitoring, developed within the MIRABLE project. The analysis focuses on two domains: the thermal domain, using Sensirion SHT45 and SEN55 temperature sensors; and the Indoor Air Quality (IAQ) domain, using an Infineon photoacoustic spectroscopy (PAS)-based sensor for carbon dioxide (CO_2). All tests were conducted under controlled laboratory conditions using calibrated reference instruments. In the thermal domain, the influence of sensor integration within the device case was investigated at temperature (T) between 15 °C and 35 °C and relative humidities (RH) between 30 %rh and 60 %rh. The results revealed self-heating effects in the desk unit, causing temperature biases of up to 0.6 °C. In the IAQ domain, the repeatability and the impact of T and RH on CO_2 measurements were evaluated. T was identified as the main influencing factor; whereas, RH had a negligible effect. These results were supported by statistical analysis ANOVA. A correction strategy based on concentration intervals is proposed for operation between 15 °C and 25 °C, with an expanded uncertainty (k = 2) of (3.26–6.42) ppm for the with-case configuration. These results support the reliable use of the MIRABLE system.

Keywords: low-cost sensors; metrological characterization; thermal domain; indoor air quality; measurement uncertainty

Check for updates

Received: 19 June 2026
Revised: 17 August 2026
Accepted: 20 August 2026
Published: 23 August 2026

Copyright: © 2026 by the authors. Licensee MDPI, Basel, Switzerland. This article is an open access article distributed under the terms and conditions of the Creative Commons Attribution (CC BY) license.

1. Introduction

Indoor Environmental Quality (IEQ) is a growing scientific and social concern. As people spend around 90% of their time indoors, the thermal, visual, acoustic, and air quality conditions of enclosed spaces has a significant impact on occupants' comfort, psychological health, well-being, and productivity [1,2]. Consequently, continuous monitoring of these parameters has become an indispensable tool for ensuring adequate environmental conditions in residential and commercial buildings [2]. The 2024 revision of the European Energy Performance of Buildings Directive (EPBD) explicitly recognizes IEQ as a key complement to energy efficiency, introducing occupant-centred metrics and promoting the

adoption of smart technologies in the built environment [3]. Thermal comfort and Indoor Air Quality (IAQ) play a central role in the parameters that contribute to the definition of IEQ. In particular, the carbon dioxide (CO_2) concentration is commonly used as an indicator of ventilation quality and air exchange [4]. The American Society of Heating, Refrigerating and Air-Conditioning Engineers (ASHRAE) has published a position paper on the role of indoor CO_2 which covers its use as a metric of IAQ and ventilation, its impacts on occupants, how concentrations are measured, and its relationship with the airborne transmission of infectious diseases [5]. ASHRAE Standard 62.1-2022 recommends keeping the stationary CO_2 concentration in an enclosed environment within a maximum limit of 700 ppm above outdoor air levels, with an operating threshold commonly set at 1000 ppm for demand-controlled ventilation systems [6]. Historically, the gold standard for CO_2 monitoring has relied on high-precision analytical instruments, such as photoacoustic spectroscopy (PAS) or non-dispersive infrared (NDIR) analysers. While these technologies can provide highly accurate, traceable measurements, their widespread deployment is limited by high acquisition costs, logistical complexity and limited scalability [7]. This has led to the rapid proliferation of low-cost sensor (LCS) networks as a practical alternative for achieving dense spatial and temporal coverage of indoor environments.

Simultaneously, the accurate measurement of air temperature in the proximity of building occupants is fundamental for the evaluation of thermal comfort in accordance with international standards such as ISO 7730 [8] and ASHRAE 55 [9]. Temperature sensors integrated into multi-sensor devices are increasingly used for this purpose; however, their deployment in compact electronics introduces self-heating artefacts that can compromise measurement accuracy if not properly characterized [10].

The development of low-cost sensor-based monitoring systems has opened new perspectives for distributed and widespread monitoring of IEQ. Continuous monitoring of IEQ plays a crucial role in improving the understanding of the main parameters that influence the health and perception of users [11]. In this context, the proliferation of low-cost Internet of Things (IoT) devices has facilitated the dissemination of integrated multi-sensor systems, which possess the capacity to simultaneously acquire multiple environmental parameters [7]. The EQ-OX and PROMET&O systems have been designed for simultaneous monitoring of multiple IEQ quantities with a low level of uncertainty and low cost [11,12].

Beyond single-parameter IAQ monitoring, low-cost sensor arrays have also been widely exploited in electronic nose (e-nose) platforms for the identification and discrimination of gases. Recent examples include the utilization of graphene-based chemiresistor arrays functionalized with metal phthalocyanines and porphyrazines for the simultaneous discrimination of ammonia, benzene, and hydrogen sulfide [13], and adaptive e-nose frameworks combining heterogeneous metal-oxide, MEMS, electrochemical, and NDIR sensors for VOC pattern recognition via multivariate analysis [14]. While these platforms target different gas species and prioritize pattern discrimination over metrological traceability, they highlight two aspects that are directly relevant to the present study: the strong dependence of low-cost sensor arrays on environmental conditions and enclosure design, and the practical need for systematic characterization strategies before such devices can be reliably deployed.

However, the spread of these sensors gives rise to important metrological questions. It is well established that such devices are generally susceptible to instrumental drift, cross-sensitivity to interfering gases, and dependence on thermo-hygrometric conditions. The consequence of these factors is an increase in measurement uncertainty and a limitation of the reliability of the collected data [15]. In distributed sensor networks, many nodes have unquantified measurement uncertainties and lack traceability to the International System of Units (SI), necessitating the development of reliable methods for assessing data quality

and measurement uncertainty in real-world environments [16]. Metrological traceability and the correct propagation of uncertainty are therefore essential requirements for any environmental monitoring system that aspires to provide comparable and reliable data.

The literature proposes several calibration methodologies for low-cost sensors measuring temperature, relative humidity, and CO_2. These approaches are generally based on simple experimental procedures and have been successfully applied over ranges of 0–50 °C for temperature, (0–90) %rh for relative humidity, and (0–1100) ppm for CO_2 concentrations [11,17]. In particular, recent studies have focused on improving the performance of low-cost CO_2 sensors through the implementation of correction algorithms and data-driven calibration techniques [18–20]. Despite these advances, the metrological characterization of multi-sensor systems remains challenging.

While several calibration methodologies have been proposed for individual low-cost sensors measuring temperature, relative humidity, and CO_2 [11,15,18], the majority of these studies characterize sensing elements in isolation, under laboratory conditions that do not reproduce the thermal and electronic interactions occurring once the sensor is integrated into a compact multi-sensor enclosure. In particular, the combined influence of enclosure-induced self-heating on temperature readings and of humidity/temperature cross-sensitivity on PAS-based CO_2 measurements has rarely been addressed within a single, traceable metrological framework applied to a fully integrated device. This gap, between single-sensor calibration studies and the actual behaviour of deployed multi-sensor systems, is the specific issue addressed in the present work, which characterizes the specific multi-sensor as an integrated unit rather than as a set of independently calibrated components.

The MIRABLE project (Measurement Infrastructure for Research on heAlthy and Zero-Energy Buildings in Novel Living Lab Ecosystems), was developed through a collaboration between Politecnico di Torino and Istituto Nazionale di Ricerca Metrologica (INRiM). The project was conceived to address these challenges. The objective of the project was to develop and validate a measurement infrastructure for monitoring IEQ and occupant–environment interactions in full-scale Living Laboratories. A distinctive feature of MIRABLE is the combination of a multi-domain monitoring approach, covering thermal, visual, acoustic, and IAQ parameters, with a rigorous metrological framework based on metrological traceability, uncertainty evaluation, and sensor characterization.

In this context, the present paper focuses on the metrological characterization of the thermal and IAQ domains of the MIRABLE multi-sensor system (MIRABLE MS). Particular attention is devoted to the characterization of low-cost temperature sensors and an Infineon PAS-based CO_2 sensor under controlled laboratory conditions. The influence of sensor enclosure, temperature, and relative humidity on measurement accuracy, repeatability, and uncertainty is investigated. It is evident from the experimental results that practical correction strategies are proposed to support the reliable deployment of low-cost multi-sensor systems for IEQ monitoring in real building applications.

2. Materials and Methods

The metrological characterization of the MIRABLE MS (developed in the PRIN Project MIRABLE, Turin, Italy) was conducted on a fully assembled prototype comprising two sub-units: the MIRABLE DESK (desktop device) and the MIRABLE CHAIR (chair-mounted device). The system integrates multiple sensors; in this study, the focus was on analyzing thermal comfort and IAQ monitoring. All characterization activities were carried out at the INRiM laboratories in Torino, Italy.

All the sensors are mounted on a custom-designed PCB developed for the MIRABLE architecture and communicate via the I2C interface.

2.1. Thermal Domain Characterization

The thermometers subjected to metrological characterization were three Sensirion SHT45 (Sensirion AG, Stäfa, Switzerland) thermo-hygrometers (two of which were installed in the chair unit and one in the desk unit) and the Sensirion SEN55 (Sensirion AG, Stäfa, Switzerland) air quality module (which was installed in the desk unit). The SHT45 sensors are specifically employed to measure air temperature in the proximity of the building occupant, while the SEN55, although primarily an air quality module, provides a temperature output that was also evaluated. The SEN55 employs a fan to enhance convective coupling between ambient air and the sensing element which was of particular interest for comparison.

The characterization was performed by comparison against two calibrated Pt100 reference thermometers (CalPower srl, Como, Italy), which were traceable to the International Temperature Scale of 1990 (ITS-90), with calibration uncertainties of 0.02 °C and 0.01 °C (k = 2) below and above 0 °C, respectively. The experiment was conducted in a programmable climatic chamber (Kambic KK-190 CHLT, Kambic d.o.o., Semič, Slovenia) to generate a controlled environment, with stable temperature and defined relative humidity (Figure 1). The measurement of interest is the air temperature inside the chamber, estimated from the averaged readings of the two reference thermometers.

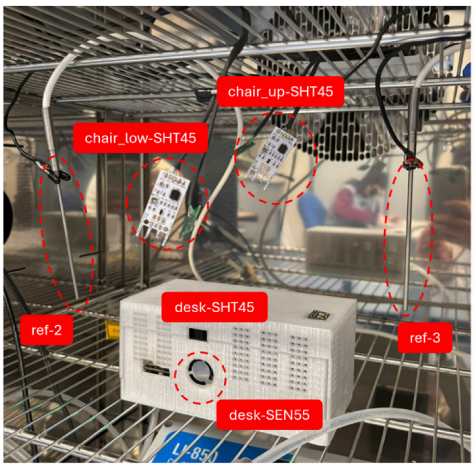


Figure 1. Experimental setup for the thermal characterization of the MIRABLE MS temperature sensors.

Two test phases were conducted. The sensors were first subjected to different temperatures between 15 and 35 °C (relative humidity 50 %rh) and compared to the references to determine the instrumental errors. Then the response of the thermometers to relative humidity was studied by varying this variable at a fixed air temperature of 23 °C. This range of T and RH was chosen as most representative of indoor environmental condition, as some research has shown that indoor comfort ranges are represented by T between 17 °C and 25 °C and associated RH from ~40 %rh to ~60 %rh [21,22]. Each test was performed in two configurations: without the external case (to characterize the intrinsic sensor performance) and with the external case (to characterize the sensor under actual operating conditions). The measurement error ε was evaluated at each set-point as:

$$\varepsilon = T_{\text{raw}} - T_{\text{ref}} \quad (1)$$

where T_{raw} is the mean sensor reading and T_{ref} is the mean reference temperature, both computed over a 2 min stability window, corresponding to 24 measurements acquired at a sampling rate of 5 s (stability criterion: peak-to-peak variation $\leq$ 0.01 °C).

The measurement uncertainty of the error (u_ε) was evaluated by considering the following uncertainty terms:

- Calibration of the reference (u_{cal}): uncertainty term that ensures the traceability of the reference sensors, equal to 0.005 °C.
- Time stability of the chamber (u_{stab}): contribution linked to the stability of the signal within the 2 min time interval, evaluated by modelling the peak-to-peak temperature difference with a uniform probability distribution.
- Uniformity of the chamber (u_{unif}): spatial uniformity of the chamber evaluated by modelling with a uniform probability distribution the maximum temperature difference in the reference sensors within the 2 min interval.
- Resolution (u_{res}): resolution of the sensor under test reported in the datasheet modelled by a uniform probability distribution.
- Repeatability (u_{repeat}): repeatability of the sensor under test evaluated as the standard deviation of measurements divided by the square root of N, that is the number of measurements within the 2 min interval.
- Reproducibility (u_{reprod}): reproducibility of the sensor under test evaluated by modelling with a uniform probability distribution the error difference observed for two independent realizations of the temperature point at 25 °C. This contribution was retrieved from the measurements without the external case, and it was added to all the uncertainty budgets related to the same sensor.

The uncertainty terms not mentioned in the above list were considered negligible for the present study.

The expanded uncertainty of the correction, U, was then calculated using a coverage factor k equal to 2, corresponding to about 95% of coverage probability.

A correction ΔT_c for each sensor was estimated by fitting the errors using a second order polynomial equation:

$$\Delta T_c = b_0 + b_1\ T_{raw} + b_2\ T_{raw}^2 \quad (2)$$

where ΔT_c denotes the temperature correction, T_{raw} is the uncorrected temperature measured by the sensor, and b_0, b_1, and b_2 are the polynomial fitting coefficients determined through least-squares regression.

2.2. Indoor Air Quality Domain Characterization

The IAQ characterization focused on the CO_2 measurement module integrated in the MIRABLE DESK. The sensor employed is the XENSIV™ PAS CO2 12 V sensor (Infineon Technologies AG, Neubiberg, Germany), which is based on the photo acoustic spectroscopy principle. Table 1 summarizes the sensor technical specifications provided by the manufacturer [23]. The characterization was performed both with and without the external case, to quantify the influence of mechanical integration on measurement performance.

Table 1. Technical specifications of the Infineon Technologies PAS CO_2 sensor.

Parameter	Value
Measurement Range	0–32,000 ppm
Specified Accuracy	±(30 ppm + 3%) within 400–5000 ppm
Communication Interface	I2C
Operating Temperature Range	0–50 °C
Operational Relative Humidity	0–85% (non-condensing)
Estimated Operational Life	10 years (at 1 measurement/min)

2.2.1. Experimental Set-Up for CO_2 Characterization

The primary characterization experiments were conducted in the QM02 "Gravimetric Mixtures and Organic Analysis Laboratory" at INRiM. The characterization was conducted within an isolator, in accordance with the procedure presented in [20]. The reference instrument that was adopted was a LI-COR LI-850 (LI-COR, Inc., Lincoln, NE, USA) [24] non-dispersive infrared (NDIR) gas analysers, previously calibrated at INRiM and was denoted as LI-cor1. The MIRABLE sensor (with or without-case, depending on the test configuration) was installed within the isolator, together with a thermo-hygrometric probe by DeltaOHM (Padova, Italy) that was installed to monitor ambient conditions, and a 5 V fan to ensure gas homogeneity.

Pure nitrogen (N_2, grade 6.0, Air Liquide, Milan, Italy) was used as the zero gas. A certified reference mixture of CO_2 in synthetic air at 396.9 ppm (gravimetrically prepared at INRiM, in accordance with the International Standard ISO 6142-1 [15]) was used as span calibration gas for both LI-COR instruments. A second reference mixture of CO_2 in N_2 at 80,325 ppm (gravimetrically prepared at INRiM) was used for generating target concentrations inside the container by dynamic dilution. The gas flow was regulated by calibrated mass flow controllers (MFC, MKS Instruments, Andover, MA, USA) with full-scale ranges of 2000 SCCM.

The objective of this activity was to characterize the performance of the MIRABLE low-cost CO_2 sensor both with and without its case, to assess the actual operating conditions of the measurement system.

As a first step, a repeatability analysis was performed, as it is a fundamental metrological parameter describing the ability of a measurement system to provide consistent results when repeated measurements of the same quantity are carried out under identical conditions. Repeatability was evaluated through the dispersion of repeated measurements and quantified by the standard uncertainty of the mean, u, calculated as:

$$u = \frac{s}{\sqrt{n}} \tag{3}$$

where s is the standard deviation of the measurements and n is the number of observations. This quantity provides an estimate of the uncertainty associated with the average measured value and decreases as the number of measurements increases.

For each test, the average measured value, of a time interval of 3 min, was calculated after excluding transient data potentially affected by temporary instabilities during the concentration stabilization phase. The measurement differences, ΔCO_2, were then determined as the difference between the average value measured by the MIRABLE sensor and the corresponding average value measured by the reference instrument (LI-cor1):

$$\Delta CO_2 = \overline{CO_{2,\mathrm{MIRABLE}}} - \overline{CO_{2,\mathrm{LI-cor1}}} \tag{4}$$

where $\overline{CO_{2,\mathrm{MIRABLE}}}$ is the average value of measurements of the low-cost sensor, and $\overline{CO_{2,\mathrm{LI-cor1}}}$ is the average value of the LI-cor1 at the corresponding time interval of the measurement of the MIRABLE sensor.

The uncertainty associated with the correction was evaluated according to the law of propagation of uncertainty. The standard deviation of the mean for each sensor was calculated as reported in Equation (3). The combined uncertainty associated with the correction, u_c, was then obtained as:

$$u_c = \sqrt{u^2_{\mathrm{MIRABLE}} + u^2_{\mathrm{LI-cor1}}} \tag{5}$$

where u_{MIRABLE} and $u_{\mathrm{LI-cor1}}$ represent the standard uncertainties associated with the

MIRABLE sensor and the reference instrument, respectively.

The expanded uncertainty of the correction, U, was then calculated using a coverage factor k equal to 2, corresponding to a confidence level of approximately 95%.

Rather than implementing a calibration function directly within the sensor firmware, this study proposes a metrologically robust correction strategy based on preserving the raw sensor output and applying corrections during the post-processing stage. This approach ensures full transparency, traceability, and reproducibility of the data treatment, allowing the analyst to verify and, if necessary, revise the applied corrections.

The proposed correction consists of adding (or subtracting, depending on its sign) a correction term, ΔCO_2, to the raw low-cost sensor measurement. The value of ΔCO_2 is determined during the pre-deployment characterization phase and is calculated as the average correction obtained from at least three independent repetitions at the same reference concentration. Since the behaviour of low-cost sensors is not always linear, the use of a single calibration curve is not recommended. Instead, a correction table derived from the experimental characterization data should be employed.

The correction values are defined for specific concentration intervals and operating conditions representative of the intended application. Consequently, the expected measurement range should be identified before deployment, and the corresponding correction factors selected accordingly. This is particularly important because the validity of the correction is limited to the concentration and environmental ranges investigated during the characterization process. Within these limits, the proposed approach provides a more reliable representation of sensor performance while preserving metrological traceability and data integrity.

2.2.2. Experimental Set-Up for Environmental Influence Assessment

Additional experiments to evaluate the influence of temperature and relative humidity on the MIRABLE CO_2 sensor were carried out in the Applied Thermodynamics Laboratory at INRiM. These experiments were undertaken as part of the thermal domain characterization described in Section 2.1. In this configuration, the MIRABLE sensor was placed inside the chamber, while LI-cor1 was positioned externally, thus avoiding thermal interference from the instrument's own electronics. The tubes utilized for sampling were routed through sealed openings in the chamber wall, while the outlet tube was returned to the chamber interior with the objective of maintaining a closed gas circuit and ensuring constant CO_2 concentration throughout each test (Figure 2). Two calibrated Pt100 probes were installed on both sides of the MIRABLE sensor to accurately monitor local temperature conditions.

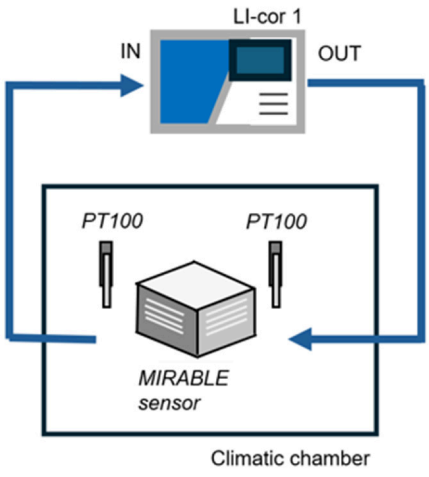


Figure 2. Scheme of the experimental set-up for the analysis of environmental influence factors on low-cost CO_2 sensor.

Temperature and relative humidity tests were performed considering the MIRABLE sensor both with and without the sensor case, in the first experiment at a constant relative humidity of 50 %rh, while varying the temperature between 15 °C and 35 °C, and in the second case at a constant temperature of 23 °C, over the range of (30–60) %rh. The experimental conditions were selected to represent typical indoor environments, including potential overheating scenarios. During all the experiments, the CO_2 concentration inside the chamber was not actively controlled; however, it was subject to continuous monitoring by the reference instrument LI-cor1, which provided the reference value for each test condition. The sensor performance was evaluated in terms of repeatability, correction, combined uncertainty, expanded uncertainty, according to Equations (3)–(5).

2.3. Statistical Analysis

The primary statistical tool applied to assess the significance of the effects of the main influence quantities on the sensor measurements was one-way analysis of variance (ANOVA). The objective of this test is to ascertain whether the means of two or more independent groups differ significantly, under the null hypothesis H_0, that all group means are equal. The test computes the F-statistic as the ratio between the between-group variance and the within-group variance [25]. A large F-statistic, associated with a p-value below the significance threshold $\alpha = 0.05$, results in the rejection of H_0, indicating that at least one pair of group means is statistically significantly different [25]. Conversely, a p-value ≥ 0.05 provides no evidence to reject H_0, and the effect of the factor under investigation is considered not statistically significant at the chosen confidence level [25].

The analysis was performed using Python 3.13.5 with NumPy 2.3.5 and pandas 2.3.3.

One-way ANOVA was applied to the following comparisons, considering a significance level $\alpha = 0.05$:

- Effect of relative humidity on temperature measurements: for the thermal domain, one-way ANOVA was used to evaluate whether the errors of the desk-SHT45, chair_up-SHT45, and chair_low-SHT45 sensors vary significantly across the tested relative humidity levels, in both the with-case and without-case configurations.
- Effect of the enclosure (with-case vs. without-case) on CO_2 measurements: for each nominal concentration level, three independent measurement series were available for each configuration. ANOVA was applied both to the individual series and to their combined mean, comparing the distribution of readings between the two configurations.
- Effect of temperature on CO_2 measurements: the sensor readings collected at different temperature set-points were compared using one-way ANOVA, separately for the with-case and without-case configurations, to determine whether temperature introduces statistically significant differences in the measured CO_2 values.
- Effect of relative humidity on CO_2 measurements: analogously, one-way ANOVA was applied to the measurements collected at different relative humidity levels at constant temperature, for both sensor configurations.

3. Results

This section presents the experimental results, organized into the thermal and IAQ domains, followed by the statistical analysis.

3.1. Thermal Domain

The metrological characteristics of the thermometers were tested in two phases. In the first phase (temperature test), sensors were exposed to five temperature set-points (15, 20, 25, 30, 35) °C at a fixed relative humidity of 50 %rh. The point at 25 °C was replicated in order to assess the short-term reproducibility. In the second phase (relative

humidity test), the temperature was fixed at 23 °C and the relative humidity varied over (30, 40, 50, 60) %rh, up to 70 %rh for the desk unit with-case.

3.1.1. Temperature Test Without External Case

Figure 3 shows the time series of temperature measurements obtained from all four sensors during the characterization process, conducted without the external case. The reference temperature T_{ref} was determined as the mean of the two Pt100 readings within each 2 min stability window. The measurement error ε, for every sensor at each set-point is reported in Table 2 as an example and in Supplementary Materials Table S1, for chair sensors.

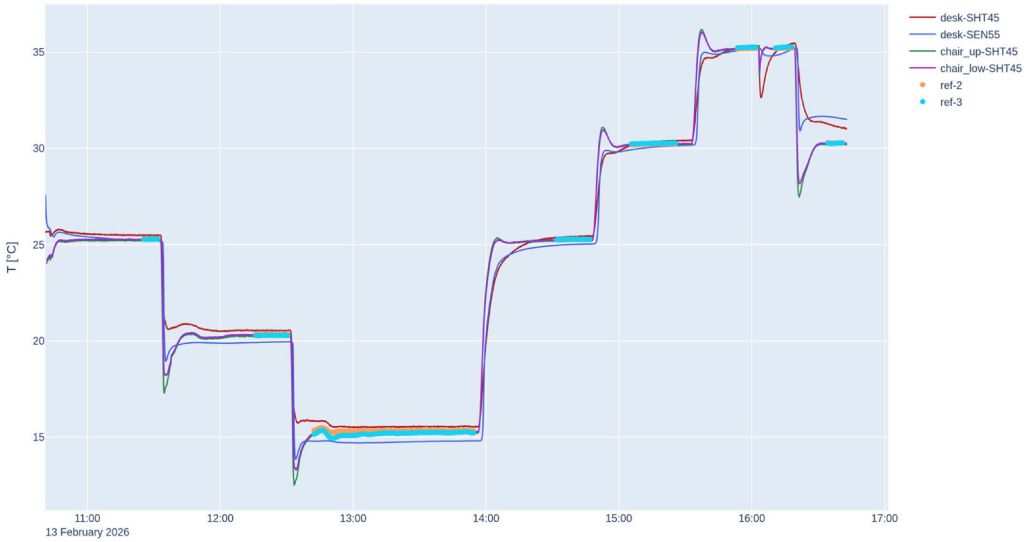


Figure 3. Time series of temperature readings from all sensors under test during the thermal characterization without the external case. The 25 °C set-point was repeated twice to assess reproducibility.

Table 2. Uncertainty budget for the two sensors on MS desk without the external case, the SHT45 and the SEN55, analysis of different *T* and same *RH* (50 %rh). Where (a) is the first measurement and (b) is the second measurement of the same point.

	15 °C		20 °C		25 °C (a)		30 °C		35 °C		25 °C (b)	
	Desk-SHT45	**Desk-SEN55**	**Desk-SHT45**	**Desk-SEN55**	**Desk-SHT45**	**Desk-SEN55**	**Desk-SHT45**	**Desk-SEN55**	**Desk-SHT45**	**Desk-SEN55**	**Desk-SHT45**	**Desk-SEN55**
T_{ref} (°C)	15.292	15.292	20.304	20.304	25.274	25.274	30.256	30.256	35.225	35.225	25.291	25.291
T_{raw} (°C)	15.548	14.780	20.535	19.945	25.428	25.027	30.389	30.122	35.288	35.150	25.490	25.195
ε (°C)	0.256	−0.512	0.231	−0.359	0.154	−0.247	0.133	−0.135	0.064	−0.075	0.199	−0.096
u_{cal} (°C)	0.005	0.005	0.005	0.005	0.005	0.005	0.005	0.005	0.005	0.005	0.005	0.005
u_{stab} (°C)	0.003	0.003	0.003	0.003	0.004	0.004	0.005	0.005	0.006	0.006	0.003	0.003
u_{unif} (°C)	0.026	0.026	0.010	0.010	0.003	0.003	0.008	0.008	0.016	0.016	0.006	0.006
u_{res} (°C)	0.001	0.001	0.001	0.001	0.001	0.001	0.001	0.001	0.001	0.001	0.001	0.001
u_{repeat} (°C)	0.002	<0.001	0.002	0.000	0.002	0.001	0.002	0.001	0.002	0.002	0.002	0.001
u_{reprod} (°C)	0.013	0.044	0.013	0.044	0.013	0.044	0.013	0.044	0.013	0.044	0.013	0.044
u_{ε} (°C)	0.030	0.051	0.017	0.045	0.015	0.044	0.017	0.045	0.022	0.047	0.016	0.045
U (°C) ($k = 2$)	0.060	0.102	0.034	0.090	0.030	0.088	0.034	0.090	0.044	0.094	0.032	0.090

For the desk-SHT45, the error is always positive ranging from 0.064 °C to 0.256 °C, with a decreasing trend with temperature. This positive bias is interpreted as a self-heating

effect: the dense PCB that hosts multiple sensing modules (thermal, CO_2, particulate matter) generates a localized heat source that increases the air temperature immediately surrounding the thermometer element. The largest uncertainty terms are those related to the spatial uniformity of the chamber and to the sensor reproducibility. This last term is particularly relevant because it is strictly related to the sensor and should be always taken into consideration while performing measurements.

The chair_up-SHT45 and chair_low-SHT45 sensors demonstrate a substantially reduced error margin, ranging from −0.079 °C to −0.059 °C and from −0.026 °C to +0.012 °C respectively. These results are in accordance with the manufacturer's accuracy specification of ±0.1 °C. The significantly reduced error compared to desk-SHT45 is consistent with the architectural difference: the chair units host only a minimal set of electronic components on a flat PCB with unobstructed heat dissipation, thus generating negligible self-heating. The uncertainty contribution from reproducibility is correspondingly an order of magnitude smaller (0.001 °C versus 0.013 °C for the desk unit), thus confirming the Sensirion SHT45 as a reliable sensor, at least in the short term. However, it is imperative to pay close attention during the design phase to avoid excessive generation of heat in its proximity.

The desk-SEN55 sensor, despite its aspirated design, intended to improve thermal coupling between ambient air and the sensing element, exhibits a significant negative bias, ranging from −0.512 °C at 15 °C to −0.075 °C at 35 °C. This negative offset is consistent with the manufacturer's stated accuracy. Furthermore, the reproducibility of the desk-SEN55 (0.044 °C) is approximately four times larger than that of the desk-SHT45 (0.013 °C), thereby confirming that the SEN55 is not well-suited for precision thermometric applications in this context (Figure 4).

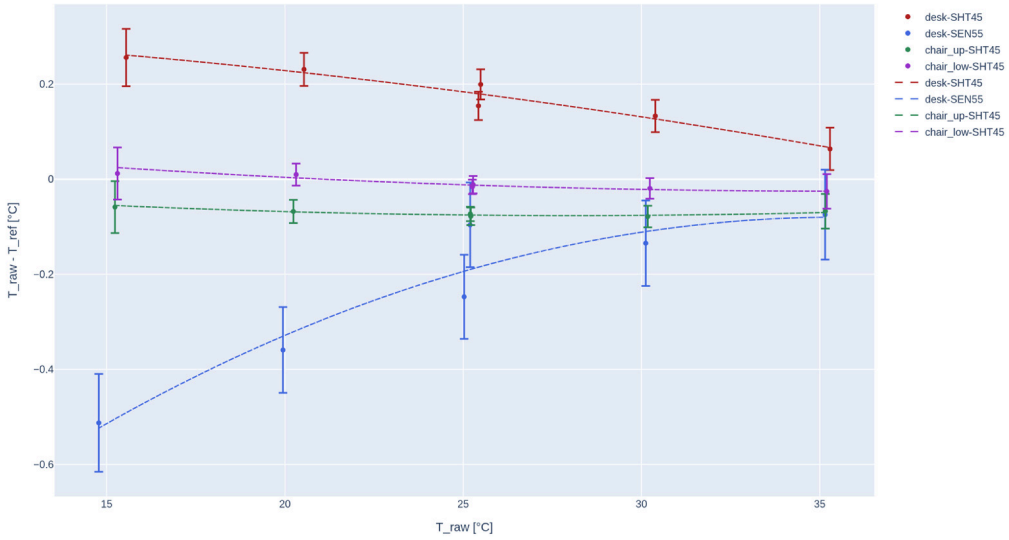


Figure 4. Measurement errors of all sensors with associated uncertainty bars (k = 2) as a function of temperature, without the external case. Dashed lines represent second-order polynomial correction curves.

For completeness, a second-order polynomial correction (Equation (2)) was fitted to the errors of each sensor in the configuration without the case. The regression coefficients are reported in Table 3. It is important to note that these corrections are valid only for the uncased configuration; as discussed in the following section, the errors change significantly when the external case is mounted, thereby rendering these corrections inapplicable to normal operating conditions.

Table 3. Regression coefficient of the polynomial correction for each tested sensor (without external case).

	b_0	b_1	b_2
desk-SHT45	−0.3238	0.0015	0.0002
desk-SEN55	1.3798	−0.0732	0.0010
chair_up-SHT45	−0.0250	0.0072	−0.0001
chair_low-SHT45	−0.1271	0.0086	−0.0001

3.1.2. Temperature Test with External Case

To better characterize the MIRABLE MS under operating conditions, other measurements were performed at 15 °C, 20 °C, 25 °C with the external case mounted. Only the desk-SHT45 and the desk-SEN55 were considered for this test since the chair units do not have an external coverage.

Table 4 report the estimated errors and the uncertainty budgets which are plotted in Figure 5.

Table 4. Uncertainty budget for the two sensors on MS desk with external case, the SHT45 and the SEN55, analysis of different *T* and same *RH* (50 %rh).

	15 °C		**20 °C**		**25 °C**	
	Desk-SHT45	**Desk-SEN55**	**Desk-SHT45**	**Desk-SEN55**	**Desk-SHT45**	**Desk-SEN55**
T_{ref} (°C)	15.330	15.330	20.330	20.330	25.288	25.288
T_{raw} (°C)	15.960	15.589	20.903	20.377	25.821	25.453
ε (°C)	0.630	0.259	0.573	0.047	0.533	0.165
u_{cal} (°C)	0.005	0.005	0.005	0.005	0.005	0.005
u_{stab} (°C)	0.005	0.005	0.004	0.004	0.003	0.003
u_{unif} (°C)	0.026	0.026	0.001	0.001	0.005	0.005
u_{res} (°C)	0.001	0.001	0.001	0.001	0.001	0.001
u_{repeat} (°C)	0.003	0.001	0.003	0.001	0.003	0.001
u_{reprod} (°C)	0.013	0.044	0.013	0.044	0.013	0.044
u_{ε} (°C)	0.030	0.051	0.015	0.044	0.016	0.044
U (°C) (k = 2)	0.090	0.102	0.030	0.088	0.032	0.088

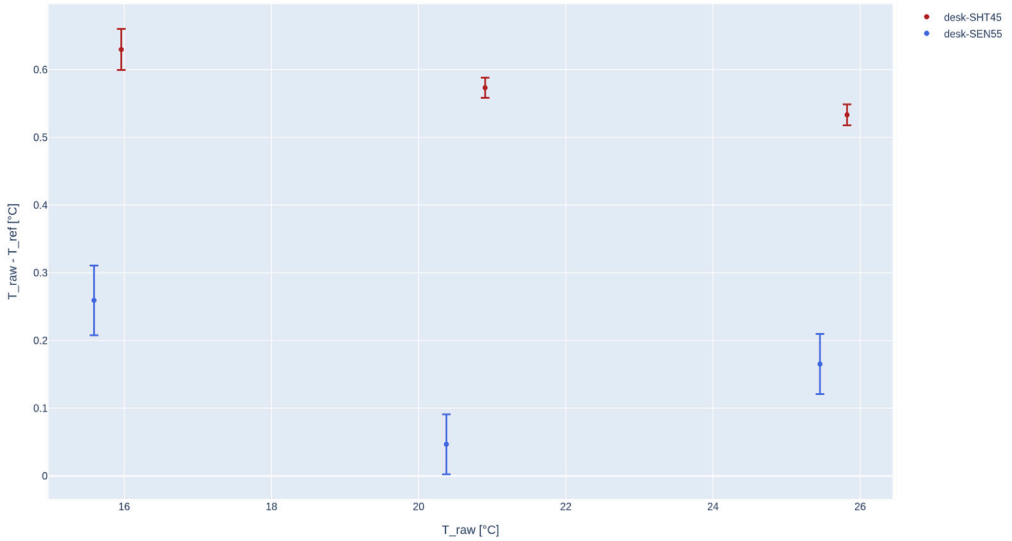


Figure 5. Measurement errors of desk-SHT45 and desk-SEN55 sensors with associated uncertainty bars (k = 2) as a function of temperature, with the external case.

For the desk-SHT45, the measurement error was found to be positive and more than double compared to the test conducted without the case, with values between ranging from 0.533 °C to 0.630 °C. This increase in error magnitude is physically consistent with the thermal insulation provided by the case, as reduced heat dissipation from the PCB creates a warmer microenvironment around the sensor. The error varies within a relatively narrow range across the three set-points (approximately 0.1 °C peak-to-peak), suggesting a predominantly additive offset rather than a strong temperature dependence, hence a correction curve is not recommended. Nevertheless, considering the application and assuming slow temperature variations around 20 °C, a conservative correction may be applied, which is $\Delta T_c = -0.6$ °C, leading to a calibration uncertainty of 0.2 °C ($k = 2$, 95%), which satisfies the project requirements for thermal comfort assessment.

For desk-SEN55, the errors in the configuration with-case are all positive (range: 0.047–0.259 °C), in contrast to the negative errors observed without the case. The additional thermal energy trapped by the case partially compensates for the natural cold bias of the SEN55. However, the poor reproducibility of this sensor (0.044 °C) remains unchanged, and no correction is proposed for this device.

3.1.3. Relative Humidity Test

The influence of relative humidity on the thermometers' performances was investigated exploiting the humidity control of the climatic chamber. The temperature was set to 23 °C and did not change during the test and relative humidity levels of (30, 40, 50, 60) %rh and additionally at 70 %rh for desk-SHT45 with-case (Tables S2 and S3). In the course of this analysis, consideration was given exclusively to the SHT45 sensors, on the basis that they had demonstrated superior performance in the previous test.

The estimated measurement errors (plotted in Figure 6 for the configuration without the case) demonstrate negligible variation with the relative humidity, meaning that the performance of the thermometers is not altered by different relative humidity conditions. The presence of minor discrepancies between the errors measured at 50 %rh (without-case) in this test and those predicted by the polynomial corrections derived from the temperature test (e.g., chair_low-SHT45: measured +0.034 °C vs. predicted −0.02 °C) serves to confirm that a stable, analytically definable correction function cannot be reliably established for these sensors. Instead, the most appropriate metrological strategy is to assign a conservative expanded uncertainty of 0.2 °C ($k = 2$, 95%) to all chair unit sensors without correction, and to apply the constant offset correction $\Delta T_c = -0.6$ °C to the desk-SHT45 with the same expanded uncertainty.

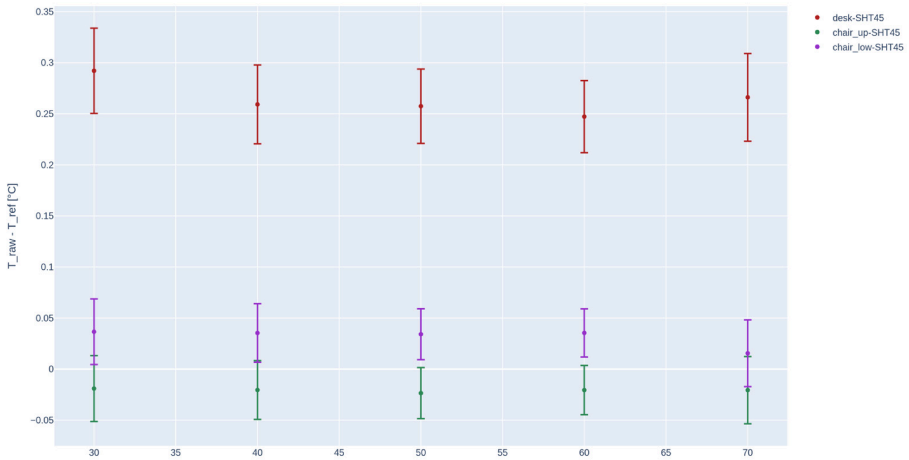


Figure 6. Measurement errors of SHT45 sensors as a function of relative humidity (without external case), at constant temperature $T = 23$ °C ($k = 2$).

The desk-SHT45 with-case at 50 %rh shows an error of 0.789 °C, consistent with the proposed correction of −0.6 °C when the associated expanded uncertainty (0.2 °C, $k = 2$) is considered. This result supports the validity of the metrological approach adopted for this sensor configuration.

3.2. IAQ Domain

This section presents the main results related to the characterization of the MIRABLE low-cost CO_2 sensor, done both in the QM02 laboratory and in the climatic chamber.

3.2.1. Characterization of the MIRABLE CO_2 Sensor in the (500−1050) ppm Range

To obtain the calibration of the sensor, measurements were conducted in a sealed isolator, thus ensuring stable concentration conditions. The data were acquired every 20 s for both the reference instrument (LI-cor1) and the MIRABLE sensor. For each concentration level, three independent measurement campaigns were conducted, both with and without the sensor enclosure, in order to ensure the reliability of the results.

Table S4 in the Supplementary Materials provides the complete uncertainty analysis over the investigated concentration range, including the mean readings, differences ΔCO_2, standard deviations, and expanded uncertainties for all six concentration levels (~500, ~600, ~700, ~800, ~900, ~1000) ppm and both sensor configurations.

The uncertainty analysis reveals several consistent patterns across the concentration range. In the without-case configuration, the MIRABLE sensor closely tracks the reference instrument at concentrations close to 500 ppm, with differences in ΔCO_2 ranging between −4.76 ppm and +4.96 ppm and expanded uncertainties U ($k = 2$) in the range of (2.0–3.8) ppm. As the nominal concentration increases, a positive systematic bias emerges and grows progressively. At 700 ppm the mean difference across the three series is approximately +6 ppm, at 800 ppm it reaches approximately +11 ppm, at 923 ppm the offset increases to values between +8 and +28 ppm (with considerable variability between series), and at around 1023 ppm the difference reaches +28 to +40 ppm. The expanded uncertainty also tends to increase at higher concentrations, reaching 6.4 ppm. This growing positive offset is consistent with the known behaviour of the PAS sensing principle, which becomes increasingly sensitive to internal thermal conditions at higher gas concentrations.

In the with-case configuration, the systematic bias is less pronounced at lower concentrations (ΔCO_2 between −7.7 ppm and +5.7 ppm at concentration between 500 ppm and 600 ppm) but increases more sharply at higher levels. At 800 ppm the mean offset is approximately +8.6 ppm, at 905 ppm it is approximately +12 ppm, and at 1017 ppm it is approximately +31 ppm. The expanded uncertainties are slightly lower than in the without-case configuration at most concentration levels; this is probably due to the damping effect of the case on short-term signal fluctuations. At 600 ppm the maximum expanded uncertainty reaches 6.4 ppm, representing the most conservative value adopted in the correction table for that interval.

An important feature of the data is the inter-series variability at certain concentration levels. At 923 ppm in the without-case configuration, for example, ΔCO_2 ranges from +8.2 ppm to +28.4 ppm across the three independent series. This indicates that the sensor response at this level is less stable and potentially more sensitive to minor fluctuations in operating conditions. This variability is reflected in the conservative approach adopted when constructing the correction table (Section 3.2.2).

3.2.2. Correction Table

The experimental data described above were used to derive a practical correction table for the MIRABLE CO_2 sensor. Given the non-monotonic behaviour of the inter-series differences and the relatively large between-series variability at certain concentration levels,

a continuous analytical function would overfit individual series and provide a false sense of accuracy, so a polynomial regression calibration curve was considered and rejected. Instead, a tabular correction approach was adopted, as this is more appropriate for a device intended for field deployment with periodic verification.

The correction value for each concentration interval was computed as the mean of the three experimental differences ΔCO_2 observed across the three independent campaigns, for each configuration. The associated uncertainty was conservatively set to the largest expanded uncertainty U measured experimentally across the three series within each interval, to ensure that the correction table provides safe coverage across realistic measurement conditions. The resulting correction table is reported in Table 5.

Table 5. Correction table for the MIRABLE CO_2 sensor. For each measurement range, the correction to be added to the raw sensor reading is reported for both configurations, together with the associated expanded uncertainty (k = 2).

MIRABLE Reading Range (ppm)	CO_2 Correction Without-Case (ppm)	CO_2 Correction With-Case (ppm)	U Without-Case (ppm)	U With-Case (ppm)
450–549	−0.29	−1.25	3.77	5.31
550–649	−2.30	−2.85	2.92	6.42
650–749	−6.01	1.22	2.30	3.98
750–849	−11.19	−8.60	5.70	4.25
850–949	−21.10	−12.25	6.42	3.26
950–1049	−34.49	−31.56	2.89	4.05

Several observations emerge from Table 5. Firstly, the correction is very small for a low-cost sensor (<3 ppm in magnitude) at the lowest concentration interval in both configurations, confirming that the sensor performs adequately without correction near typical ambient CO_2 levels. Secondly, the correction increases substantially with concentration, reaching −34.5 ppm (without-case) and −31.6 ppm (with-case) in the (950–1049) ppm interval. This progressive divergence from the reference is not linear, particularly in the without-case configuration: the jump from the (800–849) ppm interval to the (850–949) ppm interval (from −11 ppm to −21 ppm) suggests a non-linear response above approximately 800 ppm. Thirdly, the sign of the correction at 650–749 ppm differs between the two configurations (−6.01 ppm without-case vs. +1.22 ppm with-case), indicating that the enclosure modifies not only the magnitude but also the direction of the sensor offset in this specific range.

3.2.3. Influence of Temperature

The temperature dependence of the CO_2 sensor was assessed by comparing MIRABLE sensor and LI-cor1 readings at four set temperatures (15 °C, 25 °C, 30 °C, and 35 °C) and at constant relative humidity (50 %rh). The closed-circuit experimental arrangement maintained the ambient CO_2 concentration at near-ambient levels.

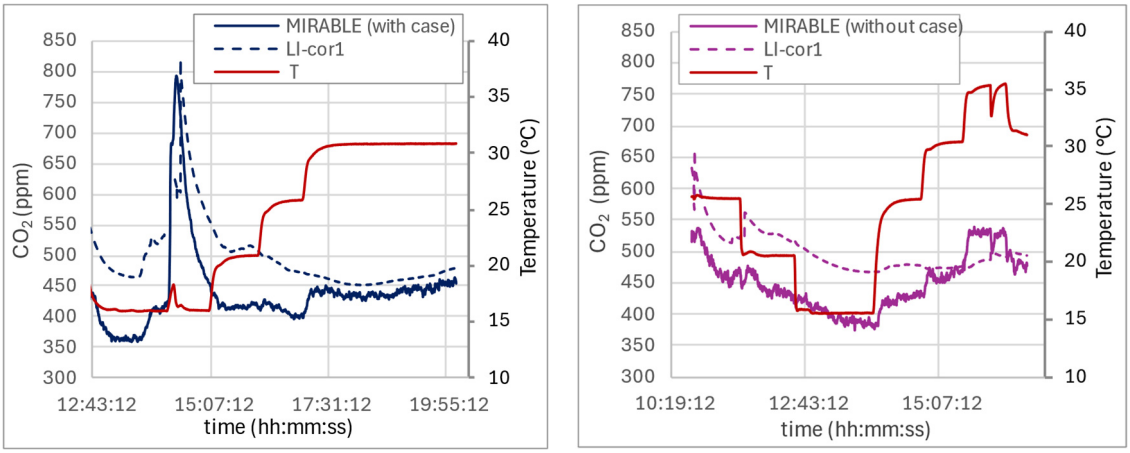
In this case, 32 MIRABLE sensor measurements (sampling every 5 s) and the corresponding LI-cor1 measurements were analyzed.

The results, reported in Table 6 and illustrated in Figure 7, reveal a strong temperature dependence of the sensor response. In the with-case configuration, the systematic offset decreases monotonically from −106 ppm at 15 °C to −16 ppm at 30 °C, indicating that the sensor progressively approaches the reference instrument reading as temperature increases. Similar behaviour is observed in the without-case configuration, but it is more pronounced: the offset reduces from −81 ppm at 15 °C and to near zero (−7 ppm) at 30 °C, but it reverses sign at 35 °C where the MIRABLE sensor over-reads the reference by approximately 49 ppm.

This reversal indicates that at 35 °C, the temperature effect dominates the sensor response, and the measured signal is no longer representative of the ambient CO_2 concentration.

Table 6. Analysis of repeatability of MIRABLE CO_2 sensor (with and without-case) at different temperatures (°C) and relative humidity (50 %rh).

	With-Case			Without-Case			
T_{ref}	15 °C	25 °C	30 °C	15 °C	25 °C	30 °C	35 °C
$\overline{CO_{2,LI-cor1}}$ (ppm)	470	480	452	472	479	474	484
$\overline{CO_{2,MIRABLE}}$ (ppm)	364	409	436	390	428	465	530
ΔCO_2 (ppm)	−106	−71	−16	−82	−50	−9	+46
$s_{LI-cor1}$ (ppm)	1.27	2.33	0.25	1.65	0.41	0.78	2.09
$s_{MIRABLE}$ (ppm)	1.85	4.35	3.24	4.57	3.21	5.63	8.71
$u_{LI-cor1}$ (ppm)	0.12	0.23	0.02	0.16	0.04	0.08	0.20
$u_{MIRABLE}$ (ppm)	0.22	0.51	0.38	0.53	0.37	0.65	1.01
u_c (ppm)	0.25	0.55	0.38	0.55	0.38	0.66	1.03
U (ppm) (k = 2)	0.50	1.11	0.75	1.11	0.75	1.32	2.07



(**a**) (**b**)

Figure 7. Comparison between MIRABLE sensor and LI-cor1 as a function of chamber temperature at constant relative humidity (50 %rh): (**a**) with-case; (**b**) without-case.

Although the ΔCO_2 values are much higher in the tests done in the climatic chamber, the uncertainties are lower than those calculated in the isolator tests.

According to the manufacturer's datasheet, the sensor's accuracy specification of ±(30 ppm + 3% of reading) is characterized at a single reference condition (T = 25 °C, RH = 30 %rh, 1013 hPa), and the documented onboard post-processing includes pressure compensation and Automatic Baseline Offset Correction for long-term drift, but no dedicated temperature-compensation algorithm [23]. In the without-case configuration, ΔCO_2 at 25 °C is −50 ppm and increases in magnitude, including a sign reversal at 35 °C. This suggests that residual, uncorrected temperature dependence of the photoacoustic signal (governed by gas density and by the thermal behaviour of the IR source, optical filter, and microphone) is the dominant contributor to the observed bias as the operating temperature departs further from the reference point.

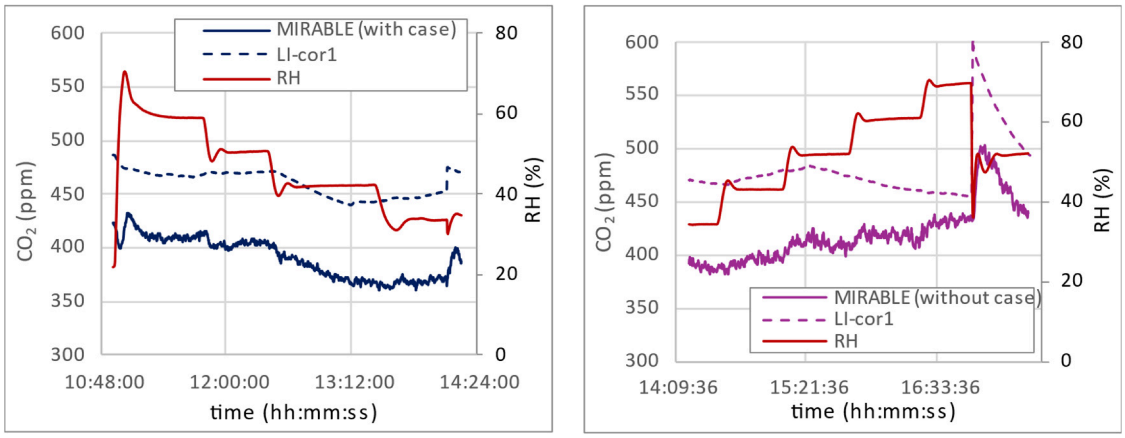
3.2.4. Influence of Relative Humidity

The influence of relative humidity on CO_2 measurements was investigated at a constant temperature of 23 °C over a range of (30–60) %rh. The results (Table 7, Figure 8) show that the MIRABLE sensor closely tracks the relative humidity variations in the reference in-

strument, in both the with-case and without-case configurations. No statistically significant dependence of the CO_2 offset on relative humidity was observed within the tested range.

Table 7. Analysis of repeatability of MIRABLE CO_2 sensor (with and without-case) at different relative humidities (%rh) and constant T (23 °C).

	With-Case				Without-Case			
RH_{ref}	60 %rh	50 %rh	40 %rh	30 %rh	60 %rh	50 %rh	40 %rh	30 %rh
$\overline{CO_{2,LI-cor1}}$ (ppm)	467	469	440	447	466	481	472	471
$\overline{CO_{2,MIRABLE}}$ (ppm)	410	405	368	367	418	412	392	393
ΔCO_2 (ppm)	−58	−65	−73	−80	−48	−69	−80	−78
$s_{LI-cor1}$ (ppm)	0.37	0.25	0.83	0.26	0.48	0.39	0.79	0.34
$s_{MIRABLE}$ (ppm)	1.58	1.52	2.45	2.02	2.99	4.02	2.39	2.82
$u_{LI-cor1}$ (ppm)	0.05	0.03	0.11	0.04	0.07	0.05	0.11	0.05
$u_{MIRABLE}$ (ppm)	0.28	0.27	0.43	0.36	0.53	0.71	0.42	0.50
u_c (ppm)	0.28	0.27	0.45	0.36	0.53	0.71	0.44	0.50
U (ppm) (k = 2)	0.57	0.54	0.89	0.72	1.06	1.43	0.87	1.00



(**a**) (**b**)

Figure 8. Comparison between MIRABLE sensor and LI-cor1 as a function of relative humidity at T = 23 °C: (**a**) with-case; (**b**) without-case.

For the with-case configuration, the offset ΔCO_2 ranges between −58 ppm and −80 ppm; for the without-case configuration, it ranges from −48 ppm to −80 ppm. These values are consistent with those observed at the same temperature in the correction uncertainty experiments, confirming that the systematic bias is predominantly temperature-dependent rather than humidity-driven.

3.3. Statistical Analysis of Influence Factors (ANOVA)

This section presents the main results of the Analysis of Influence.

3.3.1. Effect of RH on Temperature Measurements

The ANOVA results for the effect of relative humidity on temperature sensor errors are reported in Supplementary Materials Table S5 for the three SHT45 sensors, in both the with and without-case configuration. In the without-case configuration, desk-SHT45 and chair_low-SHT45 show statistically significant variation across humidity levels ($p < 0.05$), while chair_up-SHT45 does not. In the with-case configuration, none of the sensors show a statistically significant humidity effect (all $p \geq 0.10$), which is consistent with the self-heating from the electronics maintaining a lower effective relative humidity at the sensing element and thereby reducing sensitivity to external humidity variations.

3.3.2. Effect of the Case on CO_2 Measurements

The results of the one-way ANOVA applied to evaluate the effect of the enclosure (with-case vs. without-case) on CO_2 measurements are reported in Table S6, for each nominal concentration level from 500 to 1000 ppm. Both individual measurement series (I, II, III) and the combined mean are considered. At lower concentration levels (500 and 600 ppm), the first measurement series shows no statistically significant difference between configurations ($p = 0.551$ and $p = 0.834$, respectively), while series II and III yield $p < 0.05$, and the combined mean shows a borderline result at 500 ppm ($p = 0.047$) and a non-significant result at 600 ppm ($p = 0.324$). These results suggest that at concentrations close to the ambient background level, the repeatability variability of the MIRABLE sensor, which differs between configurations, can intermittently mask the true difference in mean response. At concentration of 700 ppm and above, ANOVA consistently returns highly significant F-statistics and $p < 0.05$ for both individual series and the combined mean. This confirms that the presence of the case produces a statistically significant effect on the measured CO_2 value. This finding is consistent with the systematic offset analysis reported in Section 3.2.1: the enclosure modifies the thermal microenvironment at the sensing element, shifting the sensor response in a measurable and statistically significant manner.

3.3.3. Effect of T on CO_2 Measurements

Applying a one-way ANOVA to the CO_2 measurements collected at different temperature set-points yields extremely large F-statistics in both configurations: $F = 201{,}834$ ($p < 0.05$) for the without-case configuration and $F = 387{,}907$ ($p < 0.05$) for the with-case configuration. These results provide overwhelming statistical evidence that temperature has a highly significant effect on the CO_2 sensor response, thus confirming and quantifying the trend already described in Section 3.2.3.

3.3.4. Effect of RH on CO_2 Measurements

For the CO_2 sensor, applying a one-way ANOVA to the measurements taken at different relative humidity levels yields a F of 23,208 ($p < 0.05$) for the without-case configuration and $F = 24{,}057$ ($p < 0.05$) for the with-case configuration. While the p-values indicate statistical significance, this result should be interpreted in context: the very large F-statistics reflect the high precision of the test (large number of measurements, small within-group variance) rather than a large practical effect. As documented in Table 7 (Section 3.2.4), the magnitude of the offset variation across humidity levels is small (approximately 20 ppm peak-to-peak) and does not follow a monotonic trend. This suggests that the observed statistical significance is partly driven by the sensitivity of the ANOVA test to small but consistent within-group fluctuations rather than by a dominant humidity effect. The practical implication, confirmed by the correction analysis, remains that relative humidity in the (30–60) %rh range has a limited operational impact on CO_2 measurement accuracy.

4. Discussion

The metrological characterization of the thermometers installed on the MIRABLE MS revealed a fundamental contrast between the two sensor deployment contexts. The chair units, which have minimal electronics on a flat, open PCB, behave in excellent agreement with manufacturer specifications, with errors within ± 0.1 °C and negligible reproducibility uncertainty. These sensors are immediately suitable for thermal comfort monitoring without the need for further correction, and a conservative expanded uncertainty of 0.2 °C ($k = 2$) can be assigned.

The desk unit presents a more complex picture. The thermal interference generated by the multi-domain PCB hosting sensors for CO_2, particulate matter, volatile organic

compounds, and temperature/humidity simultaneously creates a localized warming effect that biases the SHT45 temperature reading by up to 0.6 °C when the external case is mounted. This significantly limits the ability to assess thermal comfort, as this typically requires an accuracy of better than 0.5 °C in order to distinguish meaningfully between different ISO 7730 comfort categories.

The self-heating bias is inherently difficult to model with a single stable correction function because it depends on multiple interacting factors, such as the device's power-on history, ambient air circulation patterns, the mounting orientation of the case, and the thermal load of concurrent sensing operations. The variability observed between the two realizations of the 25 °C set-point (reproducibility term in the uncertainty budget) reflects this instability. For this reason, a constant correction ΔT_c of −0.6 °C with an expanded uncertainty of 0.2 °C was applied, as an approximation adequate for applications requiring uncertainty at the 0.2 °C level.

Regarding the desk-SEN55, the aspirated design improves gas exchange between the ambient air and the sensing element. This is beneficial for measuring CO_2 and particulate matter, but it does not provide the necessary temperature accuracy for thermal comfort applications. The negative bias (up to −0.5 °C without-case) and the high reproducibility uncertainty (0.044 °C) rule out the use of this sensor as a reliable thermometer. Its value lies in the IAQ measurement chain, not the thermal domain.

Additional studies are planned to investigate the most effective way to address the self-heating issue of the desk unit from a design perspective. One possibility would be to relocate the temperature sensor outside the main case, for example on a small auxiliary PCB mounted externally, thereby eliminating the primary source of thermal bias.

Laboratory tests on the CO_2 measurement module of the MIRABLE DESK provided a detailed metrological characterization, revealing the strengths and the limitations of the PAS-based low-cost sensor in its operational configuration.

The enclosed thermal environment shifts the sensor's internal temperature, which in turn alters the effective absorption cross-section used in the PAS algorithm. This can potentially reverse a marginal bias in a narrow concentration band. The expanded uncertainties range from 2.3 ppm to 6.4 ppm across the full table, which is consistent with the expected performance of a low-cost PAS sensor. These values are adequate for IAQ monitoring applications, where relevant decision thresholds such as the 1000 ppm level commonly used as a ventilation quality indicator are separated by margins significantly larger than the correction uncertainty.

The correction table is valid under the thermal and hygrometric conditions representative of the laboratory characterization experiments (approximately 20–25 °C and 30–60 %rh). However, its applicability outside this range is limited by the strong temperature dependence of the sensor response, as documented in Section 3.2.3. Therefore, users should apply temperature-specific adjustments when operating the MIRABLE sensor in environments with significantly different thermal conditions.

During the characterization tests performed in the isolator, measurements were acquired for approximately 20 min at each concentration level to ensure steady-state conditions were reached prior to data analysis. The experimental results showed that the sensor equipped with the enclosure required slightly longer to stabilize than the sensor without the enclosure. Consequently, under dynamic operating conditions, where the CO_2 concentration changes continuously, the enclosed sensor may exhibit larger deviations from the reference instrument due to its slower response time. This behaviour could also explain the larger ΔCO_2 values observed during the climatic chamber experiments, in which the CO_2 concentration was not actively controlled and varied naturally throughout the tests. Further investigations are currently underway to quantify the influence of the enclosure on

the sensor dynamic response of the multi-sensor and to assess its impact under realistic operating conditions.

The ANOVA results confirm the hierarchy of influential factors identified by the uncertainty analysis. Temperature is the dominant influential factor for the CO_2 sensor, while relative humidity plays a minor secondary role, with limited operational significance within the range representative of normal indoor environments. The presence of the enclosure has a statistically significant effect on CO_2 measurements at concentrations above 500 ppm, while its effect on temperature measurements primarily manifests as enhanced self-heating bias.

It should be noted that all characterization activities reported in this study were conducted under controlled laboratory conditions over an experimental period of approximately three weeks. While this duration is sufficient to characterize the metrological behaviour of the sensors at the time of measurement, it is not sufficient to assess long-term effects such as sensor ageing, signal drift or photoacoustic source degradation. The influence of these phenomena on measurement accuracy, and the consequent need for periodic recalibration, remain outside the scope of this study and have not been assessed. These aspects will be the subject of future investigations. It should be noted that the primary objective of this study is the metrological characterization and calibration of the sensors rather than their independent validation. In line with standard metrological practice, the correction tables were derived from the same experimental dataset used for characterization. This is the typical approach when establishing a calibration procedure, as the aim is to extract correction values from controlled measurements against a traceable reference. Future studies may independently validate the correction strategy under real operating conditions, including long-term field deployment.

5. Conclusions

This paper has presented a comprehensive metrological characterization of the MIRABLE multi-sensor system across two measurement domains: thermal comfort and IAQ. All experimental activities were conducted under controlled laboratory conditions against reference instrumentation traceable to national primary standards, ensuring the metrological rigour required for reliable building monitoring applications.

In the thermal domain, the main outcome is that the sensor deployment architecture has a significant influence on temperature measurement accuracy. The chair-mounted SHT45 sensors perform in full compliance with manufacturer specifications (errors within ± 0.1 °C, expanded uncertainty 0.2 °C for $k = 2$), making them directly suitable for thermal comfort assessment. In contrast, the desk-mounted SHT45 sensor is significantly affected by self-heating from the multi-domain PCB, resulting in a positive bias of up to 0.6 °C with the external case. While a conservative correction could bring the expanded uncertainty down to 0.2 °C, this would require careful assumptions about operating conditions. Despite its aspirated design, the desk-SEN55 is unsuitable for the intended use. Relocating the thermal sensor outside the main enclosure is recommended for the next prototype upgrade.

In the IAQ domain, the experimental characterization demonstrated that the MIRABLE CO_2 sensor can reliably track concentration variations within the range typically present in indoor environments. However, the case slows down the dynamic response of the low-cost CO_2 sensor, while improving the stability of the measurements under steady-state conditions. The most significant outcome of this study was the substantial impact of temperature on sensor performance. Although relative humidity had a negligible effect, the measured offset varied significantly with temperature, changing by more than 150 ppm across the investigated range. This behaviour confirms that temperature is the

dominant source of measurement uncertainty and must be considered when applying any correction procedure.

These findings suggest that using a single calibration curve is inappropriate. Instead, a correction table associated with a defined operating range would provide a more robust and transparent approach for practical applications. This strategy also preserves the traceability of the original measurements, as corrections can be applied during post-processing while maintaining access to the raw data.

Overall, this work demonstrates that rigorous metrological characterization of integrated multi-sensor systems, carried out prior to their deployment, is an essential prerequisite for ensuring data quality in smart building research. The results provide a metrological foundation for deploying MIRABLE in Living Lab environments dedicated to studying healthy, comfortable, and sustainable buildings. They also contribute to broader insights that are applicable to the wider community working on low-cost sensor integration for IEQ monitoring.

Supplementary Materials: The following supporting information can be downloaded at: https://www.mdpi.com/article/10.3390/chemosensors14090190/s1, Table S1: Uncertainty budget for the two sensors of the chair without the external case, the SHT45_up and SHT45_low, analysis of different T and same RH (50 %rh). The expanded uncertainty values are reported for $k = 2$; Table S2: Uncertainty budget for the sensor on MS desk SHT45 (with- and without-case), analysis of different RH and same T (23 °C). The expanded uncertainty values are reported for $k = 2$; Table S3: Uncertainty budget for the two sensors of the chair without external case, the SHT45_up and SHT45_low, analysis of different RH and same T (23 °C). The expanded uncertainty values are reported for $k = 2$; Table S4: Complete uncertainty analysis across this concentration range, including mean readings, differences ΔCO_2, standard deviations, and expanded uncertainties for all six concentration levels (~500, ~600, ~700, ~800, ~900, ~1000) ppm and both configurations (without- and with-case). Experimental data taken in laboratory condition in the isolator; Table S5: ANOVA test results, effect of RH on temperature measurements, with the significance level set to $\alpha = 0.05$; Table S6: ANOVA test results, effect of the case on CO_2 measurements, with the significance level set to $\alpha = 0.05$. In table <0.05 means that the result was ~0.

Author Contributions: Conceptualization, R.R., A.B. and F.R.; methodology, R.R., A.B., F.R. and M.S.; software, S.P.; validation, A.B. and F.R.P.; formal analysis, A.B. and F.R.P.; investigation, R.R., A.B. and S.P.; data curation, R.R., A.B., F.R. and M.S.; writing—original draft preparation, R.R. and A.B.; writing—review and editing, C.M., F.D., M.S., A.P., G.A., F.R. and F.F.; project administration, F.F. and F.R.; funding acquisition, F.F. All authors have read and agreed to the published version of the manuscript.

Funding: The MIRABLE Project was funded by the Italian PIANO NAZIONALE DI RIPRESA E RESILIENZA (PNRR)—Missione 4 "Istruzione e Ricerca"—Componente C2 Investimento 1.1, "Fondo per il Programma Nazionale di Ricerca e Progetti di Rilevante Interesse Nazionale (PRIN)" Decreto Direttoriale n. 104 del 2 febbraio 2022. Progetto PRIN 2022 "MIRABLE—Measurement Infrastructure for Research on heAlthy and zero energy Buildings in novel Living lab Ecosystems" Codice di progetto: 2022ZNJHHY.

Institutional Review Board Statement: Not applicable.

Informed Consent Statement: Not applicable.

Data Availability Statement: The raw data supporting the conclusions of this article are not yet published on public repository and will be made available by the authors on request.

Conflicts of Interest: The authors declare no conflicts of interest.

Abbreviations

The following abbreviations are used in this manuscript:

IEQ	Indoor Environmental Quality
IAQ	Indoor Air Quality
PAS	Photoacoustic spectroscopy
EPBD	European Energy Performance of Buildings Directive
ASHRAE	American Society of Heating, Refrigerating and Air-Conditioning Engineers
NDIR	Non-dispersive infrared analysers
IoT	Internet of Things
SI	International System of Units
MIRABLE	Measurement Infrastructure for Research on heAlthy and Zero-Energy
project	Buildings in Novel Living Lab Ecosystems
INRiM	Italian Istituto Nazionale di Ricerca Metrologica
MIRABLE MS	MIRABLE multi-sensor system
T	Temperature
RH	Relative humidity

References

1. Alongi, A.; Pacileo, L.; Shahrabani, M.M.N.; Spūdys, P.; Scoccia, R.; Mazzarella, L. Smart Sensors for Indoor Environmental Quality in Residential Smart Buildings: A Review. *Int. J. Sustain. Energy* **2025**, *44*, 2578592. [CrossRef]
2. Leo, V.D.; Speroni, A.; Ferla, G.; Cadena, J.D.B. Design and Validation of a Compact, Low-Cost Sensor System for Real-Time Indoor Environmental Monitoring. *Buildings* **2025**, *15*, 3440. [CrossRef]
3. The Energy Performance of Buildings Directive-Directive (EU) 2024/1275 | Circular Cities and Regions Initiative. Available online: https://circular-cities-and-regions.ec.europa.eu/support-materials/eu-regulations-legislation/energy-performance-buildings-directive-directive-eu?utm_source=chatgpt.com (accessed on 14 June 2026).
4. Carbon Dioxide Levels and Indoor Environmental Quality | Building Enclosure. Available online: https://www.buildingenclosureonline.com/blogs/14-the-be-blog-building-enclosure/post/91554-carbon-dioxide-levels-and-indoor-environmental-quality (accessed on 14 June 2026).
5. Kapsalaki, M. ASHRAE Position Document on Indoor Carbon Dioxide. Available online: https://www.aivc.org/news/ashrae-position-document-indoor-carbon-dioxide (accessed on 14 June 2026).
6. *Addendum x to Standard 62.1-2022*; Ventilation and Acceptable Indoor Air Quality. ANSI/ASHRAE: Peachtree Corners, GA, USA, 2022.
7. Lopes, S.; Orłowski, C.; Branco, P.; Karatzas, K.; Villena, G.; Saffell, J.; Marques, G.; Sousa, S.; Lenartz, F.; Bergmans, B.; et al. Low-Cost Sensor Systems and IoT Technologies for Indoor Air Quality Monitoring: Instrumentation, Models, Implementation, and Perspectives for Validation. *Sensors* **2025**, *25*, 7567. [CrossRef] [PubMed]
8. *UNI EN ISO 7730:2006*; Ergonomia degli Ambienti Termici—Determinazione Analitica e Interpretazione del Benessere Termico Mediante il Calcolo degli Indici PMV e PPD e dei Criteri di Benessere Termico Locale. UNI Ente Italiano Di Normazione: Milano, Italy, 2006. Available online: https://store.uni.com/uni-en-iso-7730-2006 (accessed on 5 June 2026).
9. *Standard 55*; Thermal Environmental Conditions for Human Occupancy. ASHRAE: Corners, GA, USA, 2023. Available online: https://www.ashrae.org/technical-resources/bookstore/standard-55-thermal-environmental-conditions-for-human-occupancy (accessed on 5 June 2026).
10. Eichstädt, S.; Gruber, M.; Vedurmudi, A.P.; Seeger, B.; Bruns, T.; Kok, G. Toward Smart Traceability for Digital Sensors and the Industrial Internet of Things. *Sensors* **2021**, *21*, 2019. [CrossRef] [PubMed]
11. Corona, J.; Tondini, S.; Gallichi Nottiani, D.; Scilla, R.; Gambaro, A.; Pasut, W.; Babich, F.; Lollini, R. Environmental Quality bOX (EQ-OX): A Portable Device Embedding Low-Cost Sensors Tailored for Comprehensive Indoor Environmental Quality Monitoring. *Sensors* **2024**, *24*, 2176. [CrossRef] [PubMed]
12. Fissore, V.I.; Barbaro, A.; Chiavassa, P.; Ramirez-Espinosa, G.; Puglisi, G.; Raviola, E.; Giusto, E.; Shtrepi, L.; Servetti, A.; Montrucchio, B.; et al. Development of a Multi-Sensor Device for Indoor Environmental Quality Assessment. In Proceedings of the 10th Convention of the European Acoustics Association Forum Acusticum 2023, Turin, Italy, 11–15 September 2023; pp. 251–254.
13. Freddi, S.; Vaghi, L.; Penoni, A.; Scapinello, L.; Sangaletti, L. A Minimal Electronic Nose Based on Graphene Functionalized with Metalated Pyrazinoporphyrazines and Phthalocyanines for Ammonia, Benzene, and Hydrogen Sulfide Discrimination. *Chemosensors* **2025**, *13*, 165. [CrossRef]

14. Gyeltshen, N.; Sanchis, A.G.; Jagannath, N.; Radaliyagoda, S.; Tobgay, S.; Hossain, M.F.; Munasinghe, K. Adaptive E-Nose: Integrating New Gas Sensors for Emerging Applications. *Sensors* **2026**, *26*, 4049. [CrossRef] [PubMed]
15. *ISO 6142-1:2015*; Gas Analysis—Preparation of Calibration Gas Mixtures. ISO: Geneva, Switzerland, 2015. Available online: https://www.iso.org/standard/59631.html (accessed on 12 January 2026).
16. Fundamental Principles of Sensor Network Metrology. Available online: https://www.euramet.org/research-innovation/search-research-projects/details/project/fundamental-principles-of-sensor-network-metrology (accessed on 14 June 2026).
17. Rivero, R.A.G.; Hernández, L.E.M.; Schalm, O.; Rodríguez, E.H.; Sánchez, D.A.; Pérez, M.C.M.; Caraballo, V.N.; Jacobs, W.; Laguardia, A.M. A Low-Cost Calibration Method for Temperature, Relative Humidity, and Carbon Dioxide Sensors Used in Air Quality Monitoring Systems. *Atmosphere* **2023**, *14*, 191. [CrossRef]
18. Cai, Q.; Zeng, N.; Yang, X.; Xu, C.; Wang, Z.; Han, P. A 30-Month Field Evaluation of Low-Cost CO_2 Sensors Using a Reference Instrument. *Atmos. Meas. Tech.* **2025**, *18*, 4871–4884. [CrossRef]
19. Müller, M.; Graf, P.; Meyer, J.; Pentina, A.; Brunner, D.; Perez-Cruz, F.; Hüglin, C.; Emmenegger, L. Integration and Calibration of Non-Dispersive Infrared (NDIR) CO_2 Low-Cost Sensors and Their Operation in a Sensor Network Covering Switzerland. *Atmos. Meas. Tech.* **2020**, *13*, 3815–3834. [CrossRef]
20. Russo, R.; Rolle, F.; Vitali, G.; Durbiano, F.; Pennecchi, F.; Pavarelli, S.; Sega, M. Metrological Characterization of Low-Cost CO_2 Sensors for Environmental Monitoring Applications. *Sensors* **2026**, *26*, 3685. [CrossRef] [PubMed]
21. Kocak, S.; Pokorádi, L. Comparison of Defuzzification Methods in The Case of Air Conditioning Systems. *Műszaki Tudományos Közlemények* **2019**, *9*, 115–118. [CrossRef]
22. Kontes, G.; Giannakis, G.; Horn, P.; Steiger, S.; Rovas, D. Using Thermostats for Indoor Climate Control in Office Buildings: The Effect on Thermal Comfort. *Energies* **2017**, *10*, 1368. [CrossRef]
23. PASCO2V01—CO_2 Sensors | Infineon Technologies. Available online: https://www.infineon.com/part/PASCO2V01 (accessed on 6 August 2026).
24. LI-COR Environmental. Available online: https://www.licor.com/products/gas-analysis/LI-830-LI-850 (accessed on 8 January 2026).
25. Fisher, R.A. *Statistical Method for Research Workers*; Springer: New York, NY, USA, 1934.

Disclaimer/Publisher's Note: The statements, opinions and data contained in all publications are solely those of the individual author(s) and contributor(s) and not of MDPI and/or the editor(s). MDPI and/or the editor(s) disclaim responsibility for any injury to people or property resulting from any ideas, methods, instructions or products referred to in the content.